Bernardo-Bermejo, S. et al., 2019. An untargeted metabolomic strategy based on liquid chromatography-mass spectrometry to study high glucose-induced changes in HK-2 cells. Journal of Chromatography A, 1596, pp.124–133.

AN UNTARGETED METABOLOMIC STRATEGY BASED ON LIQUID CHROMATOGRAPHY-MASS SPECTROMETRY TO STUDY HIGH GLUCOSE-INDUCED CHANGES IN CULTURED HUMAN PROXIMAL TUBULAR CELLS

Samuel Bernardo-Bermejo[1], Elena Sánchez-López[1], María Castro-Puyana[1,2], Selma Benito[3], Francisco Javier Lucio-Cazaña[3], María Luisa Marina[1,2*]

[1] Departamento de Química Analítica, Química Física e Ingeniería Química, Universidad de Alcalá, Ctra. Madrid-Barcelona Km. 33.600, 28871 Alcalá de Henares (Madrid), Spain.

[2] Instituto de Investigación Química Andrés M. del Río (IQAR), Universidad de Alcalá, Ctra. Madrid-Barcelona Km. 33.600, 28871 Alcalá de Henares (Madrid), Spain.

[3] Departamento de Biología de Sistemas, Universidad de Alcalá, Ctra. Madrid-Barcelona Km. 33.600, 28871 Alcalá de Henares (Madrid), Spain.

***Correspondence:** Departamento de Química Analítica, Química Física e Ingeniería Química, Universidad de Alcalá, Ctra. Madrid-Barcelona, Km. 33.600, 28871 Alcalá de Henares, Madrid, España.

E-mail: mluisa.marina@uah.es

Fax: +34-91 885 4971

Tel: +34-91 885 4935

Abstract

Diabetes mellitus is a major health concern nowadays. It is estimated that 40 % of diabetics are affected by diabetic nephropathy, one of the complications derived from high glucose blood levels which can lead to chronic loss of kidney function. It is now clear that the renal proximal tubule plays a critical role in the progression of diabetic nephropathy but research focused on studying the molecular mechanisms involved is still needed. The aim of this work was to develop a liquid chromatography-mass spectrometry platform to carry out, for the first time, the untargeted metabolomic analysis of high glucose-induced changes in cultured human proximal tubular HK-2 cells. In order to find the metabolites which were affected by high glucose and to expand the metabolite coverage, intra- and extracellular fluid from HK-2 cells exposed to high glucose (25 mM), normal glucose (5.5 mM) or osmotic control (5.5 mM glucose + 19.5 mM mannitol) were analyzed by two complementary chromatographic modes: hydrophilic interaction and reversed-phase liquid chromatography. Non-supervised principal components analysis showed a good distribution among the three groups of samples. Statistically significant variables were chosen for further metabolite identification. Different metabolic pathways were affected mainly those derived from amino acidic, polyol, and nitrogenous bases metabolism.

Keywords: diabetic nephropathy; HK-2 cells; liquid chromatography-mass spectrometry; metabolomics; multivariate analysis.

1. Introduction

Diabetes mellitus is a complicated metabolic disorder which implies insulin resistance, affected lipid metabolism, altered glucose levels, islet β-cell dysfunction, among other metabolic deregulations [1, 2]. Nowadays, diabetes is a clear worldwide health concern. In 2015, the International Diabetes Federation reported 382 million people affected by diabetes and projects a total of 592 million of diabetics by 2035 [3, 4]. Complications of diabetes mellitus are diverse and are strongly dependent on the stage of the disease. For instance, acute complications such as diabetic ketoacidosis occur at early stage of diabetes whereas chronic complications such as cerebral vascular disease, diabetic coronary artery disease or diabetic nephropathy (among others), take place at a later stage [1]. Particularly, diabetic nephropathy, which is characterized by progressive loss of kidney function, affects around 40% diabetic patients and it is the most frequent cause of end-stage kidney disease worldwide [5]. Currently, diabetic nephropathy has no known cure; thus, early diagnosis, in which discovery of biomarkers of early disease might help to stop its progression, is crucial: through identifying potential biomarkers and knowing the metabolic pathways involved, it will be possible to obtain a better understanding on the molecular mechanisms of diabetic nephropathy pathogenesis [1]. In this sense, metabolomics can help because it improves the existing knowledge on any particular disease. Metabolomics is a well-established *omics* science devoted to the study of the metabolome [6]. Specifically, non-targeted metabolomics implies the global and unbiased analysis of a specific organism, cell, or biofluid [7]. Among the analytical techniques devoted to metabolomic analysis, LC-MS is the platform of choice given its numerous advantages such as elevated robustness and sensitivity. Combination of different chromatographic modes, particularly the use of reversed-phase liquid chromatography (RPLC) together with hydrophilic interaction chromatography (HILIC)

has demonstrated to be a very useful approach to investigate a wide array of compounds having different polarities [8].

Metabolomic studies on diabetic nephropathy are diverse and are gathered in a recently published review [1]. However, to the best of our knowledge, no report exists using metabolomics analysis of an *in vitro* study (i.e. a study involving cultured cells) on diabetic nephropathy. Probably, because cell metabolomics is not as popular as the metabolomic analysis of body fluids and tissues. However, cell metabolomics provides valuable information to explain fundamental biological questions because i) it investigates how metabolic processes take place in cells, linking thereby biochemistry to cell phenotype [9-11], ii) lower levels of biological variability are expected, when compared to animal models and/or humans, because cell lines can be cultured under identical experimental conditions [11,12] and iii) cells are usually less expensive, raise no ethical concerns, and their resulting output is typically easier to interpret [9,11].

The renal proximal tubule plays a critical role in the progression of diabetic nephropathy [13]. It is widely accepted that the changes found in proximal tubular cell function in diabetic nephropathy are due to the direct effect of the diabetic microenvironment and that a high glucose (HG) microenvironment is the primary causative factor for the development of diabetic nephropathy [14]. Accordingly, there are many *in vitro* studies on the effects of HG concentrations on cultured proximal tubular cells. Thus, it would be interesting to carry out, for the first time, the metabolomic analysis of this *in vitro* model of diabetic proximal tubulopathy in order to obtain complementary information to already reported works. For this purpose, the human proximal tubular HK-2 cell line is particularly suitable because it is known to provide valuable information regarding the pathophysiology of the kidney [15]. In fact, proteomics has been used to study diabetes on HK-2 cells, providing relevant information to the understanding of

diabetic proximal tubulopathy at the protein level [16]. However, information at the small metabolite level is lacking. In this way, the aim of this work was to find potential biomarkers of diabetic nephropathy using a non-targeted metabolomics approach. To carry out this purpose, a liquid chromatography-mass spectrometry platform was developed to analyze an *in vitro* model of HG-induced metabolic alterations in HK-2 cells. In order to expand the metabolic picture, we took advantage from the fact that combination of endometabolome (intracellular metabolites) and exometabolome (metabolites excreted into the culture medium) broads the information of the cell phenotype [11]. Therefore, we planned to combine two chromatographic modes, namely RPLC and HILIC, in the analysis of both the endometabolome as well as the exometabolome of HK-2 cells exposed to HG concentrations.

2. Materials and methods

2.1. Reagents and solvents

All reagents herein used were of analytical grade or higher. Acetonitrile, methanol, ammonium acetate, and formic acid were from Thermo Fisher Scientific (Madrid, Spain). Ammonium formate was obtained from Sigma Aldrich (Madrid, Spain).

Standards purchased to carry out the metabolite identification were 2-phenylacetamide, 4-oxoproline, 5-hydroxydopamine, 5'-methylthioadenosine, adrenochrome, Ala-Gly, carbachol, cystine, D-iditol, galactitol, glutamine, glycine, glycolamide, hippuric acid, L-sorbitol, mannitol, methyl n-acetylanthranilate, N-acetyl-5-methoxykynuramine, N-acetylneuraminic acid, N-acryloylglycine, o-, m- and p-methylhippuric acid, p-acetaminobenzoic acid, phenylacetylglycine, pyridoxine, pyroglutamic acid, taurodeoxycholic acid, taurochenodeoxycholic acid, tetrahydrofolic acid and ureidoisobutyric acid and all of them were acquired in Sigma Aldrich (Madrid,

Spain) except mannitol which was obtained as a 10 % (v/v) solution from B. Braun Medical S.A. (Madrid, Spain).

2.2. HK-2 cell line culture

Human proximal tubular epithelial (HK-2) cells were purchased from the American Type Culture Collection (ATCC) (Rockville, MD, USA). HK-2 cells were maintained in DMEM/F12 supplemented with 10 % fetal bovine serum, 1 % penicillin/streptomycin/amphoterycin B, 1 % glutamine and 1 % Insulin-Transferrine-Selenium (Thermo Fisher Scientific, USA). Cells were cultured in 95 % air and 5 % CO_2 at 37 °C. One week before beginning the experiments cell culture media were changed to DMEM low glucose (5.5 mM) (ThermoFisher, Grand Island, NY).

For the metabolomics study, equal number of cells (5 x 10^5 per mL) were seeded in P35 culture dishes. In all experiments, cells were plated at 90 % confluence and when completely attached, they were treated for 24 h with medium DMEM-HG (25 mM glucose), normal glucose (5.5 mM glucose) (NG) or osmotic control (5.5 mM glucose plus 19.5 mM mannitol) (M). Seven replicates (cells cultured in different culture dishes) for each treatment were used: six for the metabolomic study itself and the remaining replicate for protein measurement and cell counting. To evaluate the amount of protein per cell, the cell number was measured manually with a hemocytometer (this method permits effective discrimination of live from dead cells using trypan blue exclusion) and the protein content per well was measured using the Pierce BCA-200 Protein Assay Kit (ThermoFisher, Grand Island, NY) according to the manufacturer's instructions. On the one hand, 110000, 160000, and 130000 cells were determined for HG, NG, and M groups, respectively. On the other hand, the protein content was 0.187, 0.365, and 0.270 mg/500 µL for HG, NG, and M groups, respectively.

144 Thereafter, all extracellular media were collected and stored at -80°C for further
145 analysis of the so-called exometabolome. Cells were washed three times with 50 mM
146 phosphate-buffered saline (pH 7.4), trypsinized and resuspended in 1 mL of the
147 appropriate culture medium. Then, cells were centrifuged at 2,500 rpm for 5 min and cell
148 pellets were stored at -80°C until further analysis of the endometabolome.
149
150 *2.3. Optimized sample preparation protocol*
151 Intracellular fluid: cell pellets from *section 2.2* were extracted with 400 µL of 75
152 % (v/v) MeOH in water, vortexed for 30 s and left still for 5 min in an ice bath followed
153 by a centrifugation step (14000*g* for 5 min at 4 ºC). The supernatant was separated into
154 two equal parts of 200 µL each and were evaporated for 3.5 h till dryness. 100 µL of 80
155 % (v/v) acetonitrile in water were added to the dried samples to be analyzed by HILIC
156 and 100 µL of water were added to the dried samples to be analyzed by RPLC, they were
157 vortexed for 30 s, centrifuged at 14000*g* for 5 min at 4 ºC and supernatants were placed
158 in glass inserts for further analyses.
159 Extracellular fluid: 300 µL of 100 % methanol were added to 100 µL of
160 extracellular fluid from *section 2.2*, vortexed for 30 s and left still for 5 min in an ice bath
161 to be then centrifuged at 14000*g* for 5 min at 4 ºC. The supernatant was then separated
162 into two equal parts of 200 µL each and the solvent was evaporated for 3.5 h. The
163 reconstitution step was the same as in the intracellular fluid.
164 QC samples were pooled by mixing the same aliquot of each sample for the
165 corresponding LC-analysis (HILIC or RPLC).
166
167 *2.4. Liquid Chromatography – Mass Spectrometry analysis*

168 Analyses were carried out using an 1100 series LC system (Agilent Technologies,
169 Germany) coupled to a 6530 series quadrupole time-of-flight (QTOF) mass spectrometer
170 (Agilent Technologies, Germany) by means of a Jet Stream orthogonal electrospray
171 ionization (ESI) source. The LC system consisted of a degasser, a quaternary pump, an
172 automatic injector, and a thermostatic column compartment. Agilent Mass Hunter
173 Qualitative Analysis software (B.07.00) was used for MS control and data acquisition.
174 Along all experiments, two reference ions were used, *m/z* 121.0509 ($C_5H_4N_4$) and *m/z*
175 922.0098 ($C_{18}H_{18}O_6N_3P_3F_{24}$) for positive ionization mode, and *m/z* 119.036 ($C_5H_4N_4$) and
176 *m/z* 1033.9881($C_{18}H_{18}O_6N_3P_3F_{24}$) for negative ionization mode. A solution containing
177 these ions was continuously infused at 15 µL min^{-1} into the system by means of a 25 mL
178 Gastight 1000 Series Hamilton syringe (Hamilton Robotics, Bonaduz, Switzerland) on a
179 NE-3000 pump (New Era Pump Systems Inc., Farmingdale, NY, USA), to allow proper
180 mass correction.

181 Analyses were carried out in a C18 Ascentis Express column (Sigma, St Louis,
182 USA), having 100 x 2.1 mm i.d. dimensions (fused-core® particles with 0.5 µm thick
183 porous shell and an overall particle size of 2.7 µm) and a HILIC (OH5) Ascentis Express
184 column (Sigma, St Louis, USA), having 100 x 2.1 mm i.d. dimensions (fused-core®
185 particles with 0.5 µm thick porous shell and an overall particle size of 2.7 µm). In both
186 cases, guard columns (5 x 2.1 mm i.d.) of the same composition as the analytical columns
187 were used. Columns were kept at 40 ºC during the analysis of the samples. An injection
188 volume of 10 µL and a flow rate of 0.4 mL min^{-1} were used.

189 Mobile phases in HILIC were water with 10 mM of ammonium formate solution
190 and 0.2 % formic acid (eluent A) and 98 % acetonitrile with 2 mM of ammonium formate
191 and 0.2 % in formic acid. The gradient in HILIC mode was from 55 % B to 100 % B in
192 30 min, 100 % B for 5 min and returned to starting conditions (55 % B) in 1 min, keeping

193 it during 15 min. Mobile phases in RPLC were water (eluent A) and acetonitrile (eluent
194 B), both with 0.1% formic acid. In RPLC mode the gradient was set as follows: 5 % B to
195 100 % B in 30 min, 100 % B for 5 min, returning to starting conditions (5 % B) in 1 min,
196 and keeping it for 15 min.

197 The ionization source conditions were: a capillary voltage of 3000 V with a nozzle
198 voltage of 0 V; nebulizer pressure at 35 psig; sheath gas of jet stream of 6.5 L min^{-1} at
199 275 ºC; and drying gas of 10 L min^{-1} at 275 ºC. The fragmentator (cone voltage after
200 capillary) was set at 125 V in HILIC and 100 V in RPLC. The skimmer and octapole
201 voltages were 60 V at 750 V, respectively. MS analyses were performed in negative ESI
202 mode in HILIC analysis and positive ESI mode in RPLC, with mass range set at *m z* 70-
203 1600 (extended dynamic range) in full scan resolution mode at a scan rate of 2 scans per
204 second.

205 MS/MS analyses for metabolite identification were carried out by selecting the
206 $[M+H]^+$ ions of the metabolites as precursor ions at the given retention time with a
207 collision energy of 20 V, except for the cases where it was not enough to fragment the
208 precursor ion, for which higher voltages were applied (30, 40 or 50 V).

209

210 *2.5. Metabolomic sequence*

211 To ensure good repeatability in the system, several blanks and QCs were
212 introduced at the beginning of the sequence. Samples were then randomized and a QC
213 was injected every six samples and at the end of the sequence.

214

215 *2.6. Data treatment and analysis*

216 Molecular features were created by the Molecular Feature Extraction tool in Mass
217 Hunter Qualitative Analysis (B.07.00) using as possible adducts, H^+, Na^+, K^+ and NH_4^+

218 in the positive ionization mode and $HCOO^-$ for the negative ionization mode. Molecular
219 features were extracted with a minimum of 9,000 counts in HILIC and 12,000 counts in
220 RPLC. These values were calculated as three times signal-to-noise (S/N) ratio.
221 Agilent Mass Profiler Professional tool (B.02.00) was employed for filtering and
222 alignment of the data. Retention time data was 0.1% with a window of 1.00 min in HILIC
223 and a window of 0.15 min in RPLC. Mass tolerance in HILIC and RPLC was 20.0 ppm
224 with a mass window of 2.0 mDa.
225 SIMCA 14.0 (Umetrics, Umeå, Sweden) was used for multivariate statistical
226 analysis. Both principal component analysis (PCA) and partial least square discriminant
227 analysis (PLS-DA) models were performed on the data after log-transformation, Pareto
228 scaling and normalization against the protein content (see *section 2.2*). Datasets are
229 available with the manuscript. Variable importance in the projection (VIP) values of the
230 first component of the PLS-DA models were used to select significant molecular features.
231 Univariate statistical analysis Mann-Whitney U test was carried out using R
232 (http://www.R-project.org) employing the Benjamini-Hochberg false discovery rate
233 (FDR) for multiple testing correction of resulting p-values.
234 Venn diagrams were created using Venny tool (version 2.1.0)
235 (http://bioinfogp.cnb.csic.es/tools/venny/index.html).
236
237 *2.7. Identification of metabolites*
238 Molecular features that showed significant differences in the PLS-DA models
239 were further subjected to the identification process. This process was carried out by
240 searching the obtained accurate mass values, assuming an error of 30 ppm, in the CEU
241 Mass Mediator database from the Centre for Metabolomics and Bioanalysis (CEMBIO,
242 Spain) [17]. This database enables the simultaneous search of metabolites in different

databases such as KEGG (https://www.genome.jp/kegg/), HMDB (http://www.hmdb.ca/), METLIN (https://metlin.scripps.edu), and LipidMaps (http://www.lipidmaps.org/). Based on their likelihood to be present in biological samples, the possible metabolites were filtered removing exogenous compounds such as drugs or compounds of plant origin.

Standards of those metabolites found in the database that were commercially available were acquired (see *section 2.1*) and were analyzed under the same analytical conditions to obtain their retention time and MS/MS fragmentation pattern. In this way, they could be used to confirm metabolite identification. In case of standards that could not be acquired, a tentative identification based on the comparison of the experimental MS/MS spectra obtained for each molecular feature and those predicted in HMDB database, CFM-ID (cfmid.wishartlab.com), and literature, was performed.

3. Results and discussion

3.1. Optimization of the sample treatment and analysis

The main objective of this work was to develop a metabolomic platform to study diabetic tubulopathy (i.e. the changes induced by HG conditions) through an *in vitro* model based on human proximal tubular HK-2 cells. As the common scenario in metabolomics studies, optimization of sample treatment and sample analysis was firstly carried out aiming to obtain as many molecular features as possible. In this sense, first, size of the Petri dishes was studied. On the one hand, large dishes could be desired since they make it possible to cultivate a larger number of cells, but, on the other hand, this implies a larger use of culture medium as well as larger incubation times, which, in turn, translates into higher experimental costs. Also, in some cases limited availability demands the use of reduced amounts of cells [18] so smaller culture dishes might be

preferred. In this study, the number of molecular features found in intracellular fluid for P35 (35 mm diameter, 10 mm height, and 11.7 cm^2 growth area) and P60 (60 mm diameter, 15 mm height, and 19.5 cm^2 growth area) was evaluated to cultivate HK-2 cells. Both HILIC and RPLC analyses were carried out, using initial conditions detailed in the supporting information. In HILIC, 178 and 224 features were found in P35 and P60, respectively, whereas that in RPLC, 206 and 267 features were found in P35 and P60, respectively. This means that, although the area in P60 was considerably larger than in P35, the number of obtained molecular features in HILIC and RPLC in P60 was not much higher than in P35. Thus, P35 was chosen as a compromise between the number of molecular features and the amount of culture medium and time of cell growth, as previously stated.

Once selected the Petri dish to grow the cells, the next step consisted on selecting the best extraction conditions to obtain information from the intracellular fluid, which includes the extraction solvent and its proportion as well as evaluating the possibility to use the process of sonication. To find the best extraction solvent which allows obtaining a greater number of intracellular molecular features, two solvents were used, ACN and MeOH in different concentrations 25, 50 and 75 % (v/v) in water. Three samples for each condition were used. In the RPLC analysis, is important to note that if the concentration of organic solvent, either ACN or MeOH, was 50 % (v/v) or lower, polymeric-like compounds with *m/z* values higher than 715 were observed between minute 11-20 (data not shown). This can be due to the fact that when using low concentration of organic solvent, the elimination of large molecules such as proteins in the samples, was not efficient. Thus, the concentrations to be compared were 75 % ACN and 75 % MeOH, selecting 75 % MeOH due to the higher number of molecular features observed with this solvent (sum of HILIC+RPLC features was 164 with ACN and 263 in MeOH).

293 The next step which was studied was the sonication process. A group of three
294 samples were placed in an ultrasound bath for 5 min and other three samples were not
295 sonicated. The number of components both in HILIC and RPLC was higher in the group
296 of samples which was not sonicated (sum of HILIC+RPLC features was 266 when
297 sonication was not used and 135 when sonication was applied). Therefore, no sonication
298 was employed in the extraction process as sonication reduced the number of features as
299 well as added an unnecessary complexity to the extraction process.
300 Once optimized the sample preparation, the next step consisted of assaying
301 different parameters related to chromatographic and detection systems. Thus, first,
302 different mobile phases were used in the HILIC and RPLC analyses. In HILIC, when
303 evaluating the number of features obtained when using a mobile phase composed of 10
304 mM ammonium acetate in water (eluent A) and 2 mM ammonium acetate in ACN (eluent
305 B) and compared to initial mobile phase conditions (see supporting information) the
306 number of features decreased to 50 thus mobile phase composed of 10 mM ammonium
307 formate and 0.2% formic acid in water as eluent A, and 2 mM ammonium formate and
308 0.2% formic acid in 95% ACN as eluent B was selected. Accordingly, in RPLC, the
309 mobile phase having 0.1 % formic acid in water (eluent A) or in ACN (eluent B) was
310 chosen as it enabled to obtain more than two times the number of molecular features than
311 when mobile phases composed of 10 mM ammonium acetate in water (eluent A) or in 95
312 % ACN (eluent B) were used.
313 Next, ionization mode (positive or negative ESI) was evaluated. Despite the fact
314 that by running both platforms (HILIC and RPLC) in positive and negative ESI modes
315 translates into a wider picture of the metabolome, a more straight-forward and realistic
316 way is to select the ionization mode more suitable for each platform under given
317 conditions. Thus, the number of features detected in both ESI modes were tested for each

318 platform. Herein, the ionization mode selected was ESI- in HILIC and ESI+ in RPLC as
319 under these conditions the number of molecular features was higher (in HILIC, 132 and
320 236 features for ESI+ and ESI-, respectively, and in RPLC, 290 and 125 features for ESI+
321 and ESI-, respectively).

322 Finally, the influence of fragmentator voltage was studied using the recommended
323 voltage for this type of compounds, 100 and 125 V. In this case, the mass accuracy was
324 taken into consideration because the voltage influence did not have much effect on the
325 number of molecular features. In the HILIC analysis 125 V was chosen because the
326 intensity of the signals increased and the mass accuracy was better. In contrast, this fact
327 was observed in the RPLC analysis with 100 V. Thus, the voltage selected was 125 and
328 100 V in HILIC and RPLC modes, respectively.

329 Once the intracellular analysis strategy was optimized, next, metabolite extraction
330 from the extracellular fluid was optimized using same analysis conditions than for the
331 intracellular fluid. The effect of metabolite extraction with MeOH and ACN was
332 evaluated both in HILIC and RPLC, using two different groups of samples of extracellular
333 fluid (ratio 1:3, extracellular fluid: organic solvent, v/v). MeOH was selected both in
334 HILIC and RPLC analysis because, in both cases, the number of metabolites extracted
335 was higher with this solvent, i.e. 66 and 127 features for HILIC and RPLC, respectively,
336 compared to 48 and 46 features found for HILIC and RPLC, respectively, when ACN
337 was used as extracting solvent.

338 **Figure 1** shows representative base peak chromatograms of intracellular (A, B)
339 and extracellular (C, D) samples analyzed both by HILIC, and RPLC, respectively. As
340 can be seen from **Figure 1**, HILIC and RPLC are two good complementary
341 chromatographic modes to analyze the different metabolites present in the two types of
342 fluids given the differences in their metabolic profiles.

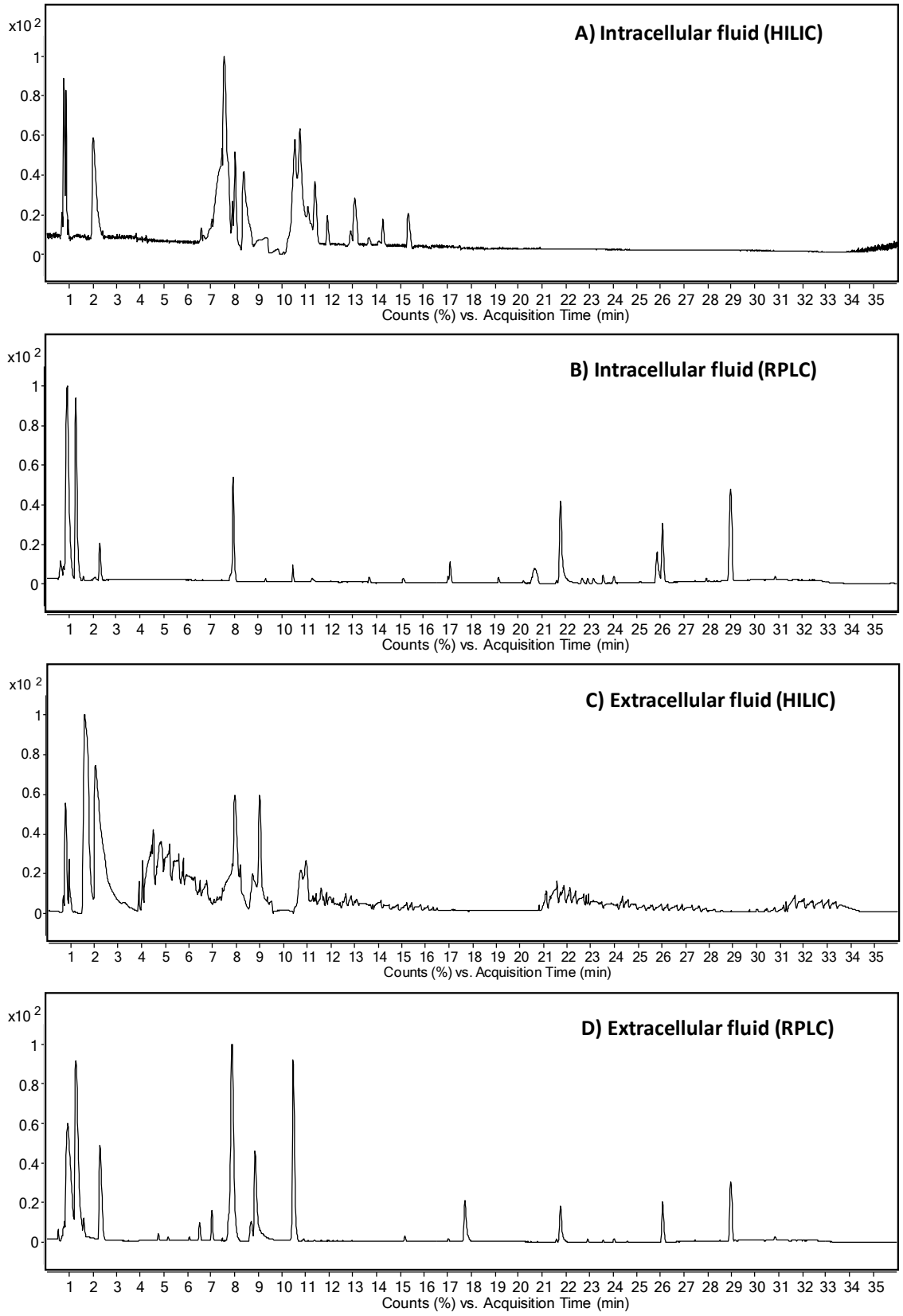

Figure 1. Base peak chromatograms of a QC sample for the four metabolomic sequences: A) intracellular fluid (HILIC), B) intracellular fluid (RPLC), C) extracellular fluid

346 (HILIC), and D) extracellular fluid (RPLC). Experimental conditions detailed on section
347 2.4.
348
349 *3.2. Non-targeted metabolomics analysis of an* in vitro *model of high glucose in HK-2*
350 *cells*
351 To carry out this study, HK-2 cells were treated either with 5.5 mM D-glucose,
352 i.e. NG, or with 25.0 mM D-glucose, i.e. HG. In order to account for changes in
353 metabolome upon differences in the osmotic pressure due to a higher glucose content in
354 the culture medium in the HG group, a third group of cells was established, the M group,
355 in which cells were treated with 5.5 mM glucose and 19.5 mM mannitol. This is a classic
356 model of diabetic nephropathy in which the effects of the diabetic environment on
357 cultured cells are studied, as seen in previous reports [19]. In all the samples, both the
358 intracellular and extracellular fluids were considered for LC analysis using two different
359 chromatographic modes, HILIC and RPLC, platforms earlier developed. Each of these
360 four sequences were constituted of the analysis of 45 samples (five biological and three
361 instrumental replicates, per three groups of samples) as well as 15 injections of the QCs
362 distributed evenly across the sequence (see *section 2.5*). Data obtained from the four
363 sequences were treated according to *section 2.6*. After molecular feature alignment and
364 filtering, the resulting datasets consisted of 108, 255, 343, and 430 variables for
365 intracellular fluid by HILIC, extracellular fluid by HILIC, intracellular fluid by RPLC,
366 extracellular fluid by RPLC, respectively.
367 As a common scenario in metabolomic studies, multivariate statistical analysis
368 was used given the complexity of the generated datasets. Thus, to prove the consistency
369 of the sequences and to observe if the three groups of samples showed significant
370 metabolic differences, unsupervised principal components analysis (PCA) was first

performed. As in previous studies on HK-2 cells [20-22], data were normalized to the protein content (determined as detailed in *section 2.2*). Note that normalization to the cell number resulted in a very similar pattern in the PCA (**Figure S1**). As can be seen in **Figure 2**, all four sequences performed well analytically as the QC samples clustered together in all cases. The PCA models excluding the QC data did not significantly change when compared to the PCA including the QC samples (see **Figure S2**). This is a very important fact because it demonstrates that the models were robust and the models were not influenced by the presence of the QCs. In all cases, high percentages (higher than 80 %) of variability were explained in the first two components. Also, in all cases, differences between the three groups of samples were clear, independently of the fluid analyzed (intracellular or extracellular) and the analytical platform used (HILIC or RPLC). When comparing the PCA models from **Figure 2** and **Figure S2**, in the analysis by HILIC the R^2X and Q^2 values were higher than the ones in the RPLC models for both fluids (intra- and extracellular). In the extracellular fluid the differences between the three groups of samples were more significant than in the intracellular fluid. Also, the PCA models for RPLC analysis show a somehow better clustering of each group than the ones for HILIC.

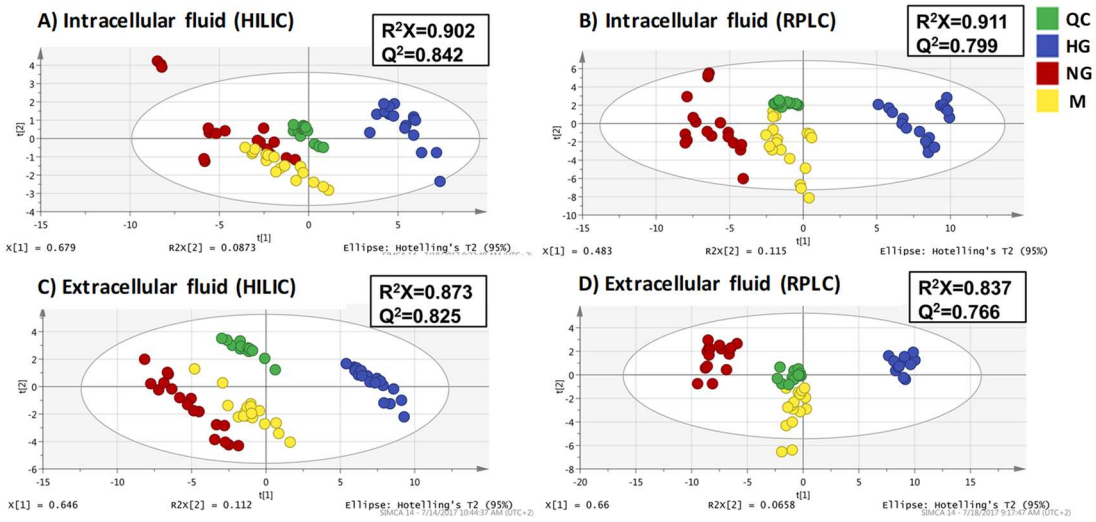

Figure 2. PCA including QC for the four analytical sequences: A) intracellular fluid (HILIC), B) intracellular fluid (RPLC), C) extracellular fluid (HILIC), and D) extracellular fluid (RPLC).

3.3. Selection of important variables

Supervised multivariate analysis (PLS-DA) was carried out comparing HG group with NG group in the four sequences in order to spot the differences in the diabetic nephropathy model. Given the difference in the osmotic pressure when the glucose concentration increases, it is required to build a second PLS-DA model, i.e. NG *vs* M group. This way, it is possible to exclude which molecular features changed due to the differences in the osmotic pressure. **Table 1** shows the parameters (R^2X, R^2Y and Q^2) and the F and p-values of the cross validated ANOVA (CV-ANOVA) for the two PLS-DA models for each analytical sequence. The largest difference between the experimental groups is given when the HG and NG groups were compared because of their high F- and low p-values. Accordingly, the fluid which showed the largest difference was the extracellular fluid. This shows the importance of analyzing this type of fluid. Next, all PLS-DA models were validated using permutation test based on 200 permutations and the results indicated that the differences were due to the differences between the samples and not due to data overfitting (**Figure S3**) [23].

Table 1. R^2X, R^2Y and Q^2 parameters and the F and p-values of the cross validated ANOVA (CV-ANOVA) for the PLS-DA models for the four analytical sequences.

PLS-DA models	R^2X	R^2Y	Q^2	CV-ANOVA	
Intracellular fluid (HILIC)					
HG vs NG	0.842	0.987	0.984	F(430.3)	$p(1.1x10^{-26})$
NG vs M	0.790	0.994	0.977	F(111.6)	$p(1.2x10^{-18})$
Intracellular fluid (RPLC)					
HG vs NG	0.649	0.994	0.988	F(561.0)	$p(2.0x10^{-28})$
NG vs M	0.492	0.995	0.984	F(216.5)	$p(1.0x10^{-22})$
Extracellular fluid (HILIC)					
HG vs NG	0.870	0.998	0.996	F(2072.3)	$p(3.7\ x10^{-37})$
NG vs M	0.686	0.986	0.980	F(338.9)	$p(4.2x10^{-25})$
Extracellular fluid (RPLC)					
HG vs NG	0.798	0.991	0.990	F(1056.2)	$p(5.0x10^{-30})$
NG vs M	0.611	0.992	0.987	F(491.8)	$p(8.69x10^{-25})$

In order to select the components which changed significantly between HG *vs* NG but did not change between NG *vs* M, the variable importance in the projection (VIP) value was selected as metrics. Those variables with VIP higher than 1.10 in the HG *vs* NG PLS-DA models which had VIP values lower than 1.10 in the NG *vs* M models were chosen as potential relevant molecular features. **Figure 3** shows the Venn diagrams of the resulting variables, where it can be seen that the number of variables is lower in the analysis by HILIC than in the analysis by RPLC.

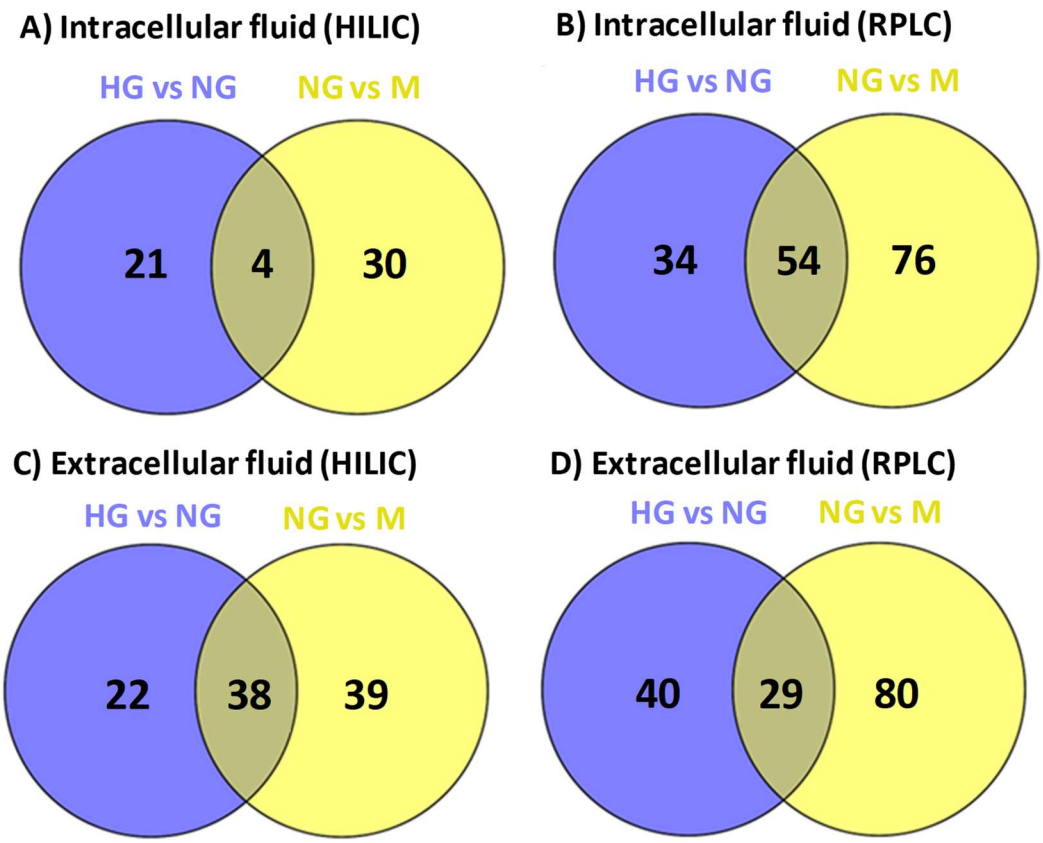

Figure 3. Venn diagrams of the four analytical sequences: A) intracellular fluid (HILIC), B) intracellular fluid (RPLC), C) extracellular fluid (HILIC), and D) extracellular fluid (RPLC).

3.4. Identification of potential biomarkers

Following the procedure described in *section 2.7*, a total of 21 and 22 statistically significant features were obtained when intracellular and extracellular fluid of HK-2 cells were analyzed by HILIC whereas that using the RPLC approach, a total of 34 and 40 molecular features were found for intracellular and extracellular fluid, respectively. The values of retention time, molecular formula, experimental *m/z* value, mass error compared to database, the main fragments obtained in the MS/MS spectra, the VIP values for the pairwise PLS-DA models, and the trend observed for all these significant metabolites are shown in **Tables 2 and S1**. As it can be seen in **Table 2**, a total of 12 metabolites were

identified when intracellular or extracellular fluids were analyzed by HILIC and RPLC. Among them, six different metabolites were unequivocally identified through confirmation with the analysis of standards. Namely, by HILIC analyses it was possible to identify sorbitol and glutamine in the intracellular fluid, and phenylacetylglycine and pyridoxine in the analysis of extracellular fluid. In addition, when RPLC was employed, hippuric acid was unequivocally identified in intracellular fluid, and 5'-methylthioadenosine and phenylacetylglycine in extracellular fluid. It is interesting to highlight that phenylacetylglycine was identified as a relevant metabolite in extracellular fluid using both HILIC and RPLC.

Table 2. Metabolites identified unequivocally and tentatively for the four analytical sequences.

#	RT (min)	Molecular formula	Identification	Monoisotopic mass (Da)	Mass error (ppm)	Main fragments (MS/MS)	VIP (p-value)**		Trend***
							HG *vs* NG	NG *vs* M	
Intracellular fluid (HILIC)									
1	2.43	$C_{10}H_{11}NO_3$	Phenylacetylglycine	193.0740	0.5	-	1.44 ($2.13 \cdot 10^{-9}$)	0.69	↑
2	7.15	$C_6H_{14}O_6$	Sorbitol*	182.0804	7.7	101.0258, 113.0257,108.9907	2.15 ($1.28 \cdot 10^{-9}$)	1.04	↑
3	7.64	$C_5H_7NO_3$	Pyroglutamic Acid	129.0439	10.1	-	1.67 ($3.19 \cdot 10^{-9}$)	0.88	↑
4	14.30	$C_5H_{10}N_2O_3$	Glutamine*	146.0693	1.4	127.0528, 109.0437, 100.9334	1.48 ($1.60 \cdot 10^{-9}$)	0.73	↓
Intracellular fluid (RPLC)									
5	3.35	$C_{11}H_{15}NO_4$	L-4-Hydroxy-3-methoxy-a-methylphenylalanine	225.1006	2.2	180.1036, 208.0892	1.47 ($8.78 \cdot 10^{-5}$)	0.50	↑
6	4.11	$C_9H_9NO_3$	Hippuric acid*	179.0584	1.1	105.0323, 77.0380, 959739, 54.9454	1.18 ($8.78 \cdot 10^{-9}$)	0.97	↑
7	27.94	$C_{23}H_{45}NO_3$	N-stearoyl valine	383.3406	1.8	324.3314	1.11 ($9.81 \cdot 10^{-5}$)	0.71	↑
Extracellular fluid (HILIC)									

8	2.53	$C_{10}H_{11}NO_3$	Phenylacetylglycine*	193.0745	3.1	117.0422, 105.0040, 132.9899	1.33 ($7.98 \cdot 10^{-10}$)	0.99	↑
9	2.78	$C_8H_{11}NO_3$	Pyridoxine*	169.0747	4.7	122.0609, 150.0555, 108.0458, 138.0562, 166.0499	1.11 ($9.11 \cdot 10^{-10}$)	0.97	↑
10	7.86	$C_{26}H_{45}NO_6S$	Taurodeoxycholic acid Taurochenodeoxycholic acid	499.3026	11.6	79.9598, 124.0105, 240.9923, 290.9857, 106.9783, 58.0294	1.30 ($1.42 \cdot 10^{-9}$)	0.26	↑
11	7.87	$C_5H_7NO_3$	Pyroglutamic Acid	129.0440	10.8	-	1.43 ($1.06 \cdot 10^{-9}$)	0.51	↑
Extracellular fluid (RPLC)									
12	0.91	$C_{12}H_{23}NO_7$	N-(1-Deoxy-1-fructosyl)isoleucine N-(1-Deoxy-1-fructosyl)leucine	293.1437	13.0	230.1366, 258.1303, 132.0978	2.78 ($8.78 \cdot 10^{-9}$)	0.64	↑
13	1.32	$C_{15}H_{21}NO_7$	N-(1-Deoxy-1-fructosyl)phenylalanine	327.1317	0.3	292.1167, 166.0843, 310.1283, 178.0836	2.51 ($9.66 \cdot 10^{-9}$)	0.0	↑
14	2.51	$C_{11}H_{15}N_5O_3S$	5'-Methylthioadenosine*	297.0895	0.3	136.0614	1.20 ($6.90 \cdot 10^{-9}$)	0.57	↑
15	5.16	$C_{10}H_{11}NO_3$	Phenylacetylglycine*	193.0745	3.1	135.0457, 107.0485, 109.9634, 120.0817	1.39 ($7.43 \cdot 10^{-9}$)	1.01	↑

*Unequivocal identification.
**p-value of Mann Whitney U test < FDR cut-off (0.020).
***↑: The metabolite (on average) is more abundant in HG vs NG; ↓: The metabolite (on average) is less abundant in NG vs M.

As it can be seen in **Table 2**, pyroglutamic acid was tentatively identified both in intra and extracellular fluids. In spite of the retention time obtained for the standard of this compound was similar to those obtained analyzing the fluids by HILIC, the MS/MS spectra did not provide relevant information since its fragmentation pattern was at the noise level probably due to the low concentration of pyroglutamic acid in the sample. This fact was also observed for phenylacetylglycine in the intracellular fluid.

Taurodeoxycholic acid or taurochenodeoxycholic acid could correspond to one of the metabolites found in extracellular fluid by HILIC since its retention time as well as its MS/MS spectrum were very similar to those obtained for the standards. However, since

463 there were no significant differences among these two isomeric compounds, its
464 unequivocal identification cannot be ensured.

465 Finally, L-4-hydroxy-3-methoxy-a-methylphenylalanine could be identified
466 because its main fragment ions matched those found in the predicted MS/MS spectra
467 found in METLIN database (https://metlin.scripps.edu), and other compounds such as N-
468 stearoyl valine, N-(1-Deoxy-1-fructosyl)isoleucine or N-(1-Deoxy-1-fructosyl)leucine,
469 and N-(1-Deoxy-1-fructosyl)phenylalanine were identified by matching their MS/MS
470 spectra to those reported in the literature [24,25].

471 Among the different metabolites from **Table S1** that could not be identified, it
472 should be indicated that some of them could be organic acids, amino acids, carbohydrates
473 and di-, tri- or tetrapeptides.

474

475 *3.5. Biological interpretation*

476 Once the identification of potential biomarkers was carried out, the next step is
477 explaining the biological relevance of the resulting metabolites. **Figures S4-S6** shows the
478 box-plots for the 15 metabolites identified either unequivocally or tentatively.

479 Regarding intracellular metabolites, seven identified metabolites were affected.
480 As can be seen in **Figures S4-S6** all of them except glutamine appear to be up-regulated
481 in the HG group when compared to the NG group. Hippuric acid is a product of amino
482 acid catabolism and it has been previously related to diabetes mellitus: urinary levels of
483 hippuric acid are reduced in diabetic nephropathy in mouse models of type-1 and type-2
484 diabetes mellitus [26]. In addition, hippuric acid has also been proposed in metabolomics
485 studies as a biomarker for the evaluation of kidney injury [27].

486 Glutamine is probably the amino acid which participates in more metabolic
487 pathways and it has a central role in proximal tubular gluconeogenesis and

ammoniagenesis, which contribute to overall glucose production and to maintenance of body acid-base balance, respectively [28]. Regarding diabetes mellitus, renal glutamine uptake is increased in streptozotozin diabetic rats [29], which is a model of type-1 diabetes mellitus. In our *in vitro* model, intracellular glutamine content was reduced in the HG group but, given that glutamine is central to many important metabolic pathways in proximal tubular cells and that it is also taken up by several amino acid transporters from the culture medium, there are many potential causes for that reduction.

Diabetes is associated with acceleration of the polyol pathway, which has been suggested to mediate the development of diabetic nephropathy. Hyperglycemia-induced activation of the polyol pathway, in which aldose reductase converts glucose to sorbitol, has been specifically demonstrated in cultured proximal tubular cells and leads to accumulation of sorbitol and to increased production of collagen (a distinctive feature of diabetic nephropathy) [30,31]. In this context, our results showing an increased sorbitol content in high glucose-exposed HK-2 cells, are in good agreement with the notion that high-glucose activates the polyol pathway in proximal tubular cells. Relation of N-stearoyl valine and L-4-Hydroxy-3-methoxy-a-methylphenylalanine with diabetes have not yet been reported in the literature.

In our study, we also investigated extracellular metabolites in the culture medium of HK-2 cells. Again, seven of the identified metabolites were found in the extracellular fluid, all of them being up-regulated in the HG group when compared to the NG group (see **Figures S5 and S6**). Pyridoxine is a non-active form of vitamin B6. The transport of vitamin B6 and other water-soluble vitamins by proximal tubular cells, is typically by entry through the luminal plasma membrane [32-34]. Inside cells, pyridoxine is converted to pyridoxal phosphate, which is a coenzyme involved in the metabolism of amino acids, carbohydrates, sphingolipids and neurotransmitters. Due to these relevant functions, and

513 to the fact that mammalian cells are not able to synthesize it, pyridoxine is a normal
514 component of mammalian cell culture media. Since pyridoxine uptake in cultured
515 proximal tubular cells is carrier mediated in nature [32-34], the increased pyridoxine
516 content found in the culture (extracellular) medium of high glucose-exposed HK-2 cells,
517 is most likely due to inhibition of its carrier-mediated uptake. Interference with the normal
518 pyridoxine proximal tubular uptake process may be relevant in the genesis and/or
519 progression of diabetic nephropathy: it has been previously found that deficiency of
520 vitamin B6 in patients with type-2 diabetes is associated with more prominent alterations
521 in incipient nephropathy [35]. Furthermore, vitamin B6 vitamer pyridoxamine (a transient
522 intermediate in enzymatic transamination reactions catalysed by pyridoxal) retards the
523 development of early renal disease in diabetic animals. Renal protection by pyridoxamine
524 in diabetes mellitus has been linked to its inhibitory effect on glucose-dependent glycation
525 reactions and the formation of advanced glycation end products, which are protein
526 modifications that contribute to the pathogenesis of vascular complications of diabetes
527 [36].

528 5-methylthioadenosine, is a sulfur-containing nucleoside which is central in the
529 purine and methionine pathways [37]. Elevated serum levels of 5-methylthioadenosine
530 have been found in the streptozotozin rat model of type-1 diabetes mellitus [38]. In
531 addition, in a metabolomics study, 5-methylthioadenosine was found to be elevated in
532 human urine from patients with late-onset type-2 diabetes mellitus and, accordingly, it
533 was proposed as a metabolic marker in these patients [39]. In this context, our current
534 results allow us to hypothesize that high glucose-induced release of 5-
535 methylthioadenosine to the extracellular medium by proximal tubular cells might explain
536 the increased urinary levels of this putative biomarker of late-onset type-2 diabetes
537 mellitus.

538 N-(1-Deoxy-1-fructosyl)leucine, N-(1-Deoxy-1-fructosyl)phenylalanine and N-
539 (1-Deoxy-1-fructosyl)isoleucine are Amadori compounds (1-amino-1-deoxykectoses),
540 intermediates from the Maillard reaction and they were present in the extracellular fluid.
541 These compounds may play an important role in the endothelial dysfunction in diabetes
542 mellitus because they can produce reactive oxygen species [40,41]. Taurodeoxycholic
543 acid or taurochenodeoxycholic acid are bile acids identified in extracellular fluid.
544 Yunpeng *et al.* carried out a metabolomic and lipidomic study about anti-obesity and anti-
545 diabetes in mice where 13 bile acids were found. Authors suggested that diabetes and
546 obesity could be improved when taurodeoxycholic acid or taurochenodeoxycholic acid,
547 among others, are reduced and tauro-β-muricholic acid is increased [42].

548 Other metabolites such as phenylacetylglycine and pyroglutamic acid have both
549 been found to change in intracellular and extracellular fluids. Phenylacetylglycine is a
550 minor metabolite of fatty acids which has been associated to renal damage in several
551 metabolomics studies [43-45]. Increased urinary amounts of phenylacetylglycine have
552 been associated with mitochondrial fatty acid β-oxidation [46]. In the present work, the
553 augmented phenylacetylglycine levels in fluid cell and in culture medium from high-
554 glucose exposed HK-2 cells, relative to those of the NG group implied that high glucose
555 might affect the lipid metabolism of proximal tubular cells. However, specific
556 experiments should be performed to confirm this hypothesis. As hippuric acid,
557 pyroglutamic acid is a product of amino acid catabolism which is also related to diabetes
558 mellitus having antidiabetic properties in type-2 diabetes in mice and rats [47].

559 To the best of our knowledge, this is the first time that a metabolomics approach
560 is used to assess HG-induced changes on HK-2 cells. However, further studies should be
561 performed to quantify accurately the magnitude of the changes in the intracellular and

562 extracellular content of the reported metabolites as well as to identify the mechanisms
563 responsible for their changes.
564
565 **4. Concluding remarks**
566 The platform based on RPLC and HILIC analysis herein developed has
567 demonstrated to be a valuable tool to obtain information from the cell phenotype (endo-
568 and exometabolome) of HK-2 cells. For the first time, an *in vitro* model of the effects of
569 HG on the metabolome of human proximal tubular cells has been evaluated. By using
570 multivariate analysis both non-supervised (PCA) and supervised (PLS-DA) methods,
571 clear differentiation between experimental groups of samples was observed. Statistically
572 significant molecular features were selected based on their VIP values and they were
573 identified. According to our study, the unequivocally identified metabolites
574 characteristics of diabetic nephropathy are hippuric acid, glutamine, sorbitol, pyridoxine,
575 5'-Methylthioadenosine and phenylacetylglycine which are involved in different
576 metabolic pathways such as polyol, purine, methionine, phenylalanine and tyrosine
577 metabolism. Also, pyroglutamic, L-4-hydroxy-3-methoxy-a-methylphenylalanine, N-
578 stearoyl valine, N-(1-Deoxy-1-fructosyl)isoleucine or N-(1-Deoxy-1-fructosyl)leucine,
579 N-(1-Deoxy-1-fructosyl)phenylalanine, taurodeoxycholic acid or taurochenodeoxycholic
580 acid and pyroglutamic acid were tentatively identified.
581
582 *Acknowledgments*
583 Authors thank the Ministry of Economy and Competitiveness (Spain) for research
584 project CTQ2016-76368-P. S.B.B and M.C.P. thank the same Ministry for their
585 predoctoral (BES-2017-082458) and "Ramón y Cajal" (RYC-2013-12688) research
586 contracts, respectively. E.S.L. thanks the Comunidad of Madrid (Spain) and European

587 funding from FEDER program (project S2013/ABI3028, AVANSECAL-CM) for her
588 contract.

589 **5. References**

590 [1] Wu T, Qiao S, Shi C, Wang S, Ji G. Metabolomics window into diabetic
591 Complications. J Diabetes Investig. 2018;9:244-55.

592 [2] Testa R, Bonfigli AR,Genovese S, De Nigris V, Ceriello A. The possible role of
593 flavonoids in the prevention of diabetic complications. Nutrients. 2016;8:1–13.

594 [3] International Diabetes Federation (IDF). 2013. http://www.idf.org/diabetesatlas.
595 Accessed July 2018.

596 [4] Hugill AJ, Stewart ME, Yon MA, Probert F, Cox IJ, Hough TA, Scudamore CL,
597 Bentley L, Wall G, Wells SE, Cox RD. Loss of arylformamidase with reduced thymidine
598 kinase expression leads to impaired glucose tolerance. Biol Open. 2015;4:1367–75.

599 [5] Gross JL., de Azevedo MJ, Silveiro SP, Canani LH, Caramori ML, Zelmanovitz T.
600 Diabetic Nephropathy: Diagnosis, Prevention, and Treatment, Diabetes Care.
601 2005;28:164-76.

602 [6] Klupczyńska A, Dereziński P, Kokot ZJ. Metabolomics in medical sciences - Trends,
603 challenges and perspectives. Acta Pol Pharm. 2015;72:629-41.

604 [7] Kohler I, Verhoeven A, Derks RJ, Giera M. Analytical pitfalls and challenges in
605 clinical metabolomics. Bioanalysis. 2016;8:1509-32.

606 [8] Bi H, Krausz KW, Manna SK, Li F, Johnson CH, González FJ. Optimization of
607 harvesting, extraction, and analytical protocols for UPLC-ESI-MS-based metabolomic
608 analysis of adherent mammalian cancer cells. Anal Bioanal Chem. 2013;405:5279-89.

609 [9] Zhang A, Sun H, Xu H, Qiu S, Wang X. Cell Metabolomics. OMICS. 2013;17:495-
610 501.

611 [10] León Z, García-Cañaveras JC, Donato MT, Lahoz A. Mammalian cell
612 metabolomics: experimental design and sample preparation. Electrophoresis.
613 2013;34:2762-75.

614 [11] Hounoum BM, Blasco H, Emond P, Mavel S. Liquid chromatography-high-
615 resolution mass spectrometry-based cell metabolomics: experimental design,
616 recommendations, and applications. TrAC – Trend. Anal. Chem. 2016; 75: 118-28.
617 [12] Cuperlovic-Culf M, Barnett DA, Culf AS, Chute I. Cell culture metabolomics:
618 applications and future directions. Drug Discov. Today. 2010;15:610-21.
619 [13] Gilbert RE. Proximal Tubulopathy: Prime Mover and Key Therapeutic Target in
620 Diabetic Kidney Disease. Diabetes 2017;66:791–800.
621 [14] Bonventre JV. Can We Target Tubular Damage to Prevent Renal Function Decline
622 in Diabetes?. Semin Nephrol. 2012;32:452–62.
623 [15] Ryan MJ, Johnson G, Kirk J, Fuerstenberg SM, Zager RA, Torok-Storb B. HK-2: an
624 immortalized proximal tubule epithelial cell line from normal adult human kidney.
625 Kidney Int. 1994;45:48-57.
626 [16] So EJ, Kim HJ, Kim CW. Proteomic analysis of human proximal tubular cells
627 exposed to high glucose concentrations. Proteomics Clin Appl. 2008;2;1118-26.
628 [17] Gil de la Fuente A, Godzien J, Fernández López M, Rupérez FJ, Barbas C, Otero A.
629 Knowledge-based metabolite annotation tool: CEU Mass Mediator. J Pharm Biomed
630 Anal. 2018;154:138-149.
631 [18] Luo X, Li L. Metabolomics of Small Numbers of Cells: Metabolomic Profiling of
632 100, 1000, and 10000 Human Breast Cancer Cells. Anal Chem. 2017;89:11664-71.
633 [19] Aluksanasuwan S, Khamchun S, Thongboonkerd S. Targeted functional
634 investigations guided by integrative proteome network analysis revealed significant
635 perturbations of renal tubular cell functions induced by high-glucose. Proteomics.
636 2017;17:1700151.

637 [20] Liu X, Liu Y, Cheng M, Xiao H. Acute nephrotoxicity of aristolochic acid in vitro:
638 metabolomics study for intracellular metabolic time-course changes. Biomarkers.
639 2016;21:233-42.
640 [21] Zhao X, Sun K, Lan Z, Song W, Cheng L, Chi W, Chen J, Huo Y, Xu L, Liu X,
641 Deng H, Siegenthaler JA, Chen L. Tenofovir and adefovir down-regulate mitochondrial
642 chaperone TRAP1 and succinate dehydrogenase subunit B to metabolically reprogram
643 glucose metabolism and induce nephrotoxicity. Sci Rep. 2017;7:46344.
644 [22] Cheng L, Ge M, Lan Z, Ma Z, Chi W, Kuang W, Sun K, Zhao X, Liu Y, Feng Y,
645 Huang Y, Luo M, Li L, Zhang B, Hu X, Xu L, Liu X, Huo Y, Deng H, Yang J, Xi Q,Zhang
646 Y, Siegenthaler JA, Chen L. Zoledronate dysregulates fatty acid metabolism in renal
647 tubular epithelial cells to induce nephrotoxicity. Arch Toxicol. 2018;92:469-85.
648 [23] Saccenti E, Hoefsloot HCJ, Smilde AK, Westerhuis JA, Hendriks MMWB.
649 Reflections on univariate and multivariate analysis of metabolomics data. Metabolomics.
650 2014;10:361-74.
651 [24] Tan B, O'Dell DK, Yu YW, Monn MF, Hughes HV, Burstein S, Walker JM.
652 Identification of endogenous acyl amino acids based on a targeted lipidomics approach.
653 J Lipid Res. 2010;51:112-19.
654 [25] Davidek T, Kraehenbuehl K, Devuaud S, Robert F, Blank I. Analysis of Amadori
655 Compounds by High-Performance Cation Exchange Chromatography Coupled to
656 Tandem Mass Spectrometry. Anal Chem. 2005;77:140-47.
657 [26] Stec DF, Wang S, Stothers C, Avance J, Denson D, Harris R, Voziyan P. Alterations
658 of urinary metabolite profile in model diabetic nephropathy. Biochem Biophys Res
659 Commun. 2015;456:610-14.

660 [27] Gu L, Shi H, Zhang R, Wei Z, Bi KS, Chen XH. Simultaneous Determination of
661 Five Specific and Sensitive Nephrotoxicity Biomarkers in Serum and Urine Samples of
662 Four Drug-Induced Kidney Injury Models. J Chromatogr Sci. 2017;55:60-8.
663 [28] Stumvoll M, Perriello G, Meyer C, Gerich J. Role of glutamine in human
664 carbohydrate metabolism in kidney and other tissues. Kidney Int. 1999;55:778-92.
665 [29] Brosnan JT, Man KC, Hall DE, Colbourne SA, Brosnan ME. Interorgan metabolism
666 of amino acids in the streptozotocin-diabetic ketoacidotic rat. Am J Physiol.
667 1983;244:151-8.
668 [30] Bleyer AJ, Fumo P, Snipes ER, Goldfarb S, Simmons DA, Ziyadeh FN. Polyol
669 pathway mediates high glucose-induced collagen synthesis in proximal tubule. Kidney
670 Int. 1994;45:659–66.
671 [31] Lanaspa MA, Ishimoto T, Cicerchi C, Tamura Y, Roncal-Jimenez CA, Chen W,
672 Tanabe K, Andres-Hernando A, Orlicky DJ, Finol E, Inaba S, Li N, Rivard CJ, Kosugi
673 T, Sanchez-Lozada LG, Petrash JM, Sautin YY, Ejaz AA, Kitagawa W, Garcia GE,
674 Bonthron DT, Asipu A, Diggle CP, Rodriguez-Iturbe B, Nakagawa T, Johnson RJ.
675 Endogenous Fructose Production and Fructokinase Activation Mediate Renal Injury in
676 Diabetic Nephropathy, J Am Soc Nephrol. 2014;25:2526–38.
677 [32] Bowman BB, McCormick DB. Pyridoxine uptake by rat renal proximal tubular cells.
678 J Nutr. 1989;119:45-9.
679 [33] Zhang ZM, McCormick DB. Uptake of N-(4'-pyridoxyl)amines and release of
680 amines by renal cells: A model for transporter-enhanced delivery of bioactive
681 compounds. Proc Natl. Acad. Sci USA. 1991;88:10407-10.
682 [34] Said HM, Ortiz A, Vaziri ND. Mechanism and regulation of vitamin B(6) uptake by
683 renal tubular epithelia: studies with cultured OK cells. Am J Physiol Renal Physiol.
684 2002;282:465-71.

685 [35] Nix WA, Zirwes R, Bangert V, Kaiser RP, Schilling M, Hostalek U, Obeid R.
686 Vitamin B status in patients with type 2 diabetes mellitus with and without incipient
687 nephropathy. Diabetes Res Clin Pract. 2015;107:157-65.
688 [36] Voziyan PA, Hudson BG. Pyridoxamine as a multifunctional pharmaceutical:
689 targeting pathogenic glycation and oxidative damage. Cell Mol Life Sci. 2005;62:1671-
690 81.
691 [37] Avila MA, Garcıa-Trevijano ER, Lu SC, Corrales FJ, Mato JM.
692 Methylthioadenosine. Int J Biochem Cell Biol. 2004;36:2125–30.
693 [38] Zhang Y, Wang P, Xu Y, Meng X, Zhang Y. Metabolomic Analysis of Biochemical
694 Changes in the Plasma of High-Fat Diet and Streptozotocin-Induced Diabetic Rats after
695 Treatment with Isoflavones Extract of Radix Puerariae. Evid Based Complement Alternat
696 Med. 2016; 4701890.
697 [39] Tam ZY, Ng SP, Tan LQ, Lin CH, Rothenbacher D, Klenk J, Boehm BO, SPC Team,
698 ActiFE Study Group. Metabolite profiling in identifying metabolic biomarkers in older
699 people with late-onset type 2 diabetes mellitus. Sci Rep. 2017;7:4392.
700 [40] Sánchez CF, Peiró C, Rodríguez L. Los productos de amadori como mediadores de
701 disfunción endothelial en la diabetes mellitus. Endocrinol Nutr. 2004;51:497-505.
702 [41] Davidek T, Kraehenbuehl K, Devuaud S, Robert F, Blank I. Analysis of Amadori
703 Compounds by High-Performance Cation Exchange Chromatography Coupled to
704 Tandem Mass Spectrometry. Anal Chem. 2005;77:140-7.
705 [42] Qi Y, Jiang C, Cheng J, Krausz KW, Li T, Ferrell JM, Gonzalez FJ, Chiang JY. Bile
706 acid signaling in lipid metabolism: metabolomic and lipidomic analysis of lipid and bile
707 acid markers linked to anti-obesity and anti-diabetes in mice. Biochim Biophys Acta.
708 2015;1851:19-29.

709 [43] Wang Z, Xu R, Shen G, Feng J. Metabolic Response in Rabbit Urine to Occurrence
710 and Relief of Unilateral Ureteral Obstruction. J Proteome Res. 2018;17:3184-3194.
711 [44] Chen S, Zhang M, Bo L, Li S, Hu L, Zhao X, Sun C. Metabolomic analysis of the
712 toxic effect of chronic exposure of cadmium on rat urine. Environ Sci Pollut Res Int.
713 2018;25:3765-3774.
714 [45] Zhao YY, Tang DD, Chen H, Mao JR, Bai X, Cheng XH, Xiao XY. Urinary
715 metabolomics and biomarkers of aristolochic acid nephrotoxicity by UPLC-
716 QTOF/HDMS. Bioanalysis. 2015;7:685-700.
717 [46] Tanaka T, Hine DG, West-Dull A, Lynn TB. Gas-chromatographic method of
718 analysis for urinary organic acids. I. Retention indices of 155 metabolically important
719 compounds. Clin Chem. 1980;26:1839–46.
720 [47] Yoshinari O, Igarashi K. Anti-diabetic effect of pyroglutamic acid in type 2 diabetic
721 Goto-Kakizaki rats and KK-Ay mice, Br J Nutr. 2011;106:995−1004.